ELSEVIER

The Spine Journal 10 (2010) 1098–1105

THE SPINE JOURNAL

Basic Science

The effects of needle puncture injury on microscale shear strain in the intervertebral disc annulus fibrosus

Arthur J. Michalek, PhD[a], Mark R. Buckley, PhD[b], Lawrence J. Bonassar, PhD[c], Itai Cohen, PhD[b], James C. Iatridis, PhD[a,*]

[a]*School of Engineering, University of Vermont, 301 Votey Building, Burlington, VT 05405, USA*
[b]*Department of Physics, Cornell University, 109 Clark Hall, Ithaca, NY 14853, USA*
[c]*Department of Biomedical Engineering and Sibley School of Mechanical and Aerospace Engineering, Cornell University, 105 Upson Hall, Ithaca, NY 14853, USA*

Received 11 May 2010; revised 26 August 2010; accepted 23 September 2010

Abstract

BACKGROUND CONTEXT: Needle puncture of the intervertebral disc (IVD) is required for delivery of therapeutic agents to the nucleus pulposus and for some diagnostic procedures. Needle puncture has also been implicated as an initiator of disc degeneration. It is hypothesized that needle puncture may initiate IVD degeneration by altering microscale mechanical behavior in the annulus fibrosus (AF).

PURPOSE: Quantify the changes in AF microscale strain behavior resulting from puncture with a hypodermic needle.

STUDY DESIGN: Cadaveric IVD tissue explant study.

METHODS: Annulus fibrosus explants from bovine caudal IVDs that had been punctured radially with hypodermic needles were loaded in dynamic sinusoidal shear while being imaged with a confocal microscope. Digital image analysis was used to quantify local tissue strain and damage propagation with repeated shearing.

RESULTS: Needle puncture changed the distribution of microscale shear strains in the AF under load from homogenous (equal to far field) to a distinct pattern of high (4× far field) and low (0.25× far field) strain areas. Repeated loading did not cause further growth of the disruption beyond the second cycle.

CONCLUSIONS: Needle puncture results in a drastic alteration of microscale strain behavior in the AF under load. This alteration may directly initiate disc degeneration by being detrimental to tissue-cell mechanotransduction.

Keywords: Intervertebral disc; Needle puncture; Confocal; Radon transform

Introduction

The intervertebral disc (IVD) is the largest avascular organ in the body, making it susceptible to degeneration and slow to repair [1]. Needle injection into the IVD is commonly used in discography for diagnostic purposes [2,3] and is important for therapeutic [4–8] procedures, including growth factor injection and cell therapies. However, there is somewhat of a paradox as needle punctures are also commonly used to induce degeneration in the IVD. In animal models, these injuries affect both annulus integrity and nucleus pressurization [9] and can result in an acute loss of disc height [4,10–13], axial stiffness [12,14–16], and rupture pressure [17] as well as progressive structural changes consistent with degenerative disc disease [13,18–20]. More recently, discography procedures performed on nondegenerative discs have been shown to increase the risk of later degeneration [21]. It has been suggested that small relative needle sizes (ie, needle diameter relative to total IVD height) will result in a negligible effect on IVD mechanics, whereas large relative needle sizes have greater effects [14].

FDA device/drug status: not applicable.

Author disclosures: none.

This work was made possible by funding from NIH (1R01AR051146 and R21AR054867), NASA/VSGC (NNX07AK92A), and NSF (DMR-0606040), and technical assistance from Dr David Warshaw.

* Corresponding author. School of Engineering, University of Vermont, 301 Votey Bldg, 33 Colchester Ave., Burlington, VT 05405, USA. Tel.: (802) 656-2774; fax: (802) 656-1929.

E-mail address: james.iatridis@uvm.edu (J.C. Iatridis)

1529-9430/$ - see front matter © 2010 Elsevier Inc. All rights reserved.
doi:10.1016/j.spinee.2010.09.015

To date, there has been no investigation into microscale mechanics surrounding needle punctures in the IVD, which is essential for developing techniques to minimize or repair these injuries.

There is a reason to believe that microscale structural disruption after a needle puncture of the annulus fibrosus (AF) plays a role in initiating the degenerative cascade. In bovine IVDs cultured under axial compression, localized cell death has been observed in the AF in the proximity of a needle puncture [12]. Classical elasticity theory proposes that if an object with a focal defect is placed under load, the material surrounding that defect will be subjected to local strains different from those far away from the defect [22]. Intervertebral disc cells are known to be metabolically sensitive to tissue strain conditions, with low levels promoting matrix protein production but high levels leading to apoptosis [23–28]. Taken together, this suggests a scenario where altered strain patterns in the AF at the site of a needle puncture lead to structural disruption and altered cell metabolism or death.

It has been suggested that a primary cause of IVD degeneration is the accumulation of microfailure damage [29]. More recent research into interlamellar connectivity, however, indicates that the AF structure has complex interlamellar connectivity, making it particularly robust and likely effective at arresting the propagation of injuries under physiological loading [30–32]. Additionally, there is some indication that chemical cross-linking agents are able to restore mechanical function to damaged discs [33–35], although it is unclear whether these results reflect changes in all parts of the tissue [36] or a targeted repair. Furthermore, without a clear indication of how injury disrupts microscale fiber mechanics, it is difficult to design optimally effective repair techniques.

Knowledge of how the AF structure responds mechanically to injury at the microscopic level is essential to developing both effective repair strategies and less invasive diagnostic and therapeutic procedures. Based on our current understanding of AF tissue mechanics, we hypothesize that needle puncture will result in altered microscale shear strains under tissue loading; chemical cross-linking will inhibit some of this alteration; and a puncture injury will not propagate under physiological levels of applied shear strain. These hypotheses were tested using a combination of dynamic shear loading of punctured AF tissue explants, confocal microscopy, and image processing techniques, including Radon transform and feature tracking algorithms.

Methods

Mechanical testing

Twenty-two samples of AF tissue were taken from the IVDs of three bovine tails within 24 hours of sacrifice. After removal of surrounding muscle and ligaments, the four quadrants of each disc (anterior, posterior, left, and right) were each systematically assigned to one of the three experimental groups and were either punctured radially with a 21-G (n=9) or 26-G (n=12) hypodermic needle or assigned to an unpunctured control group (n=1). These needle sizes were chosen to bind those most commonly used in discography procedures [3]. Quadrants assigned to the 26- and 21-G groups were punctured radially to a depth of 15 mm with hypodermic needles (BD Precision Glide, Franklin Lakes, NJ, USA; regular bevel) at the disc midplane. On retraction of the needles, the puncture site was irrigated with approximately 20 μL of either phosphate-buffered saline (PBS) (n=11) or an aqueous solution of fluorescently labeled microspheres (Constellation; Invitrogen, Carlsbad, CA, USA) (n=6). The addition of microspheres into the PBS was a technical refinement to improve our ability to positively identify puncture sites. The microspheres had electrostatic attraction to the tissue and consequently were not expected to influence the reported measurements by interfering with the tissue staining. One additional disc was punctured in all four quadrants with a 26-G needle and irrigated with 20 μL of genipin (1% in PBS) (n=4). After storage overnight at 4°C to ensure cross-linking activity, the IVDs were removed from their adjacent vertebrae, and the AF quadrants were separated and frozen. The frozen tissue explants were cut into rectangular blocks of approximately 7 mm in length, 5 mm in height, and 5 mm in depth (Fig. 1) using a cryostat to ensure smooth parallel faces. The exact height of the specimen at the time of cutting was measured and recorded.

Before testing, the tissue specimens were thawed and stained with 5-dichlorotriazinylaminofluorescein [30,37,38] for 30 minutes followed by a 30-minute rinse in PBS. Specimens were then attached to the grips of a tissue deformation imaging stage (Harrick Scientific, Pleasantville, NY, USA) in the circumferential orientation using cyanoacrylate [39]. The imaging stage was mounted on a confocal microscope

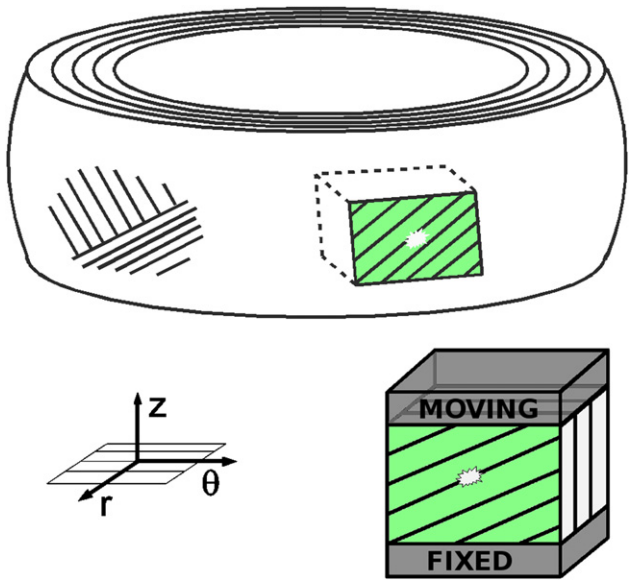

Fig. 1. Schematic showing tissue test specimen with fixed and moving boundary conditions in relation to bovine caudal disc geometry. Shading indicates imaged surface.

(Zeiss, Thornwood, NY, USA; LSM 5LIVE) with the specimen immersed in PBS. Once the puncture site was located on the specimen and centered within the microscope field of view, a series of marker lines were bleached onto the tissue surface in alignment with the gradient (z) direction using a 488-nm laser at 90 mW for 1 minute. Sinusoidal shear strain was then applied at a frequency of 0.05 Hz and an amplitude of 5% of the measured specimen height. This strain amplitude corresponds to approximately 1.7° of axial torsion in the human lumbar IVD, which is within normal physiological limits [40,41]. Displacement control was selected to most closely create tissue shears resulting from active trunk rotation rather than passive torque. During loading, images of the specimen were captured at a rate of 15 frames per second.

Strain mapping

Micrographs of needle puncture injuries were assessed both qualitatively and quantitatively to describe specific injury patterns. Quantitative assessment consisted of two-dimensional shear strain fields surrounding the puncture injuries calculated from one full cycle of loading following 10 cycles of preconditioning. This analysis used a Radon transform technique carried out in a custom-written Matlab (Mathworks, Natick, MA, USA) code as outlined in Fig. 2. This parallel projection integral transform is typically used in inverse form for tomographic reconstruction and is also useful for identifying the angle of orientation of line features in an image [42]. First, the positions of the photobleached marker lines in each frame were estimated based on a sinusoidal function fit to their positions in the unstrained and maximum positive- and negative-strained states. Before strain measurement, each image was contrast adjusted to flatten intensity gradients resulting from imaging artifacts. Along each line, a series of 94 41×41 pixel subwindows with a 36-pixel overlap were located for angular measurement. This window size was determined to provide the best possible spatial resolution without compromising the precision of angular measurements. For each subwindow (highlighted box in Fig. 2, Left), the image within it was filtered using an unsharp mask with periodic boundaries to emphasize the marker line feature. A circular mask was then applied to the subimage to attenuate edge effects. A Radon transform was performed on the subimage for angles ranging from 160° to 200°, with a resolution of 0.3°, where 180° corresponds to a vertically oriented line (Fig. 2, Right Top). This range was chosen to avoid interference from fiber bundle line features with a typical orientation of 130° or 240°. The variance of the transform was taken across the length dimension (Fig. 2, Right Bottom), with the angle (φ) at which variance was maximum indicating the orientation of the marker line. This procedure was validated on a set of test images of lines with known angles of orientation, confirming a measurement precision of 0.3°. Average shear strain in the subwindow was then calculated as $\tan(180-\varphi)$. To remove artifacts from dirt particles and poor focus, angle measurements were rejected if they fell outside of $180°\pm10°$, leaving a range of approximately ±0.17 shear strain. After strain analysis, a sine function was fit to the time history of the shear strain in each subwindow, the amplitude of which was stored for further analysis. On most of the specimens, photobleached lines ran across areas of tissue in which the surface was not on the same focal plane as the rest of the tissue in the field of view. To determine whether unfocused subwindows might introduce bias into the distribution of strain measurements, the Radon transform algorithm was also run on 2,000 41×41 pixel images of random noise. Shear measurements of random noise images showed a distinct bias toward shear strain values below 0.015 and subwindows for which

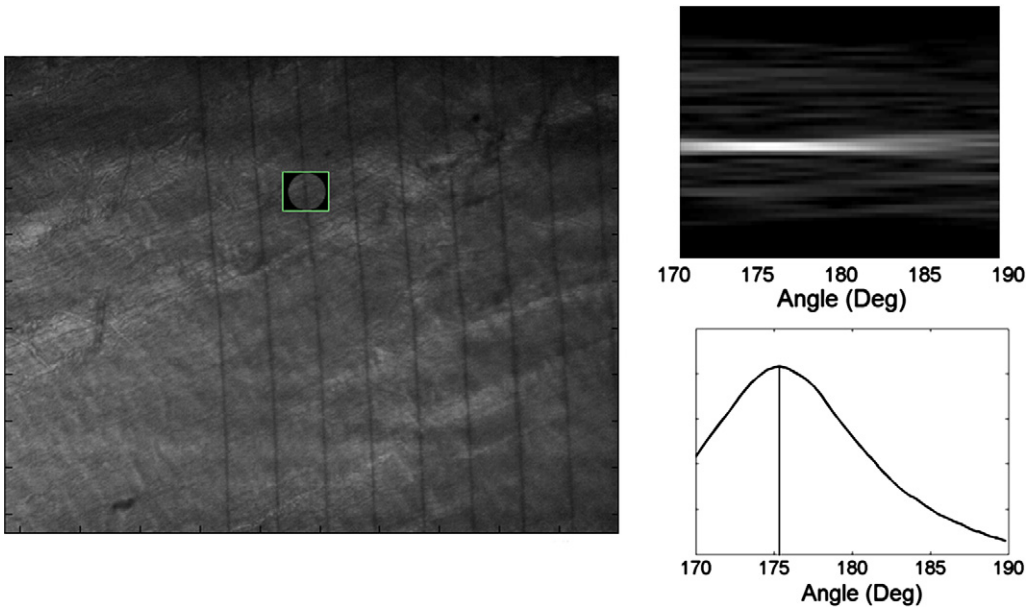

Fig. 2. Outline of Radon transform analysis of control specimen showing (Left) full image with subimage and circular mask centered on marker line, (Right Top) Radon transform of subimage, and (Right Bottom) variance of Radon transform with maximum indicating angle of marker line orientation.

the shear strain amplitude was below this value were thus excluded.

Feature tracking

To evaluate local damage propagation, two-dimensional cross-correlation was used to track four tissue features through each test from the beginning of shearing. One-dimensional correlation of displacement in the velocity (θ) direction was then used to test the assumption that if a defect is growing in size, a feature on the surface of the tissue will not be displaced along the same path during two successive cycles of shear loading. If the defect is not growing, then displacement through cycles n and n+1 will have a correlation coefficient of one. Features were defined by four 31×31 pixel regions of interest placed near the puncture site on the first frame of each image series. As the resulting correlation coefficient data were not normally distributed, they were compared between groups and cycles using a two-sided Mann–Whitney test, with $p<.05$ determining significance.

Results

In all of the measurements made, there was no distinguishable difference between the four 26-G genipin irrigated and eight 26-G specimens irrigated with saline or microspheres. They have thus been pooled for analysis.

Survey

Qualitative analysis of the confocal micrographs showed a distinct effect of needle puncture. In images of the control specimen (Fig. 3, Top), the photobleached marker lines remained straight and parallel under applied shear strain. Minimal discontinuity was observed along the lines as they crossed the boundaries between fiber bundles (inset in Fig. 3, Top). In punctured specimens, the shape and size of the injury varied greatly but typically fell into one of two categories; a circular hole with an elongated split between fiber bundles (Fig. 3, Middle) with holes approximately 100-μm diameter or a jagged tear with broken fibers visible (Fig. 3, Bottom) stretching more than 500 μm. In the control specimen, marker lines remained continuous across fiber bundle boundaries under applied shear. An increase in marker line discontinuity was observed around puncture injuries. Injury type did not correlate with needle size or anatomical location of puncture. Under applied shear, punctured specimens showed an increase in marker line discontinuity across fiber bundle boundaries in the vicinity of the puncture site (insets in Fig. 3, Middle and Bottom).

Strain mapping

Eleven of the tissue specimens (control, n=1; 26 G, n=7; 21 G, n=3) yielded images of a high enough quality for strain mapping. The control specimen (Fig. 4, Left) showed a reasonably homogenous strain field at maximum displacement. Punctured specimens (Fig. 4, Right) showed much more variation with small areas of high shear strain at fiber bundle boundaries (white arrows) and larger areas of strain less than the applied value of 0.05 within fiber bundles. Distributions of local shear strain amplitudes in all subwindows of all specimens show a distinct trend with injury (Fig. 5). Needle puncture resulted in a decrease in subwindows with shear strain close to the applied value of 0.05 and an increase in measurements at higher and lower strains. Weibull fit parameters (Table) show all scale parameters increasing and shape parameters decreasing with needle puncture, accompanied by an increase in strain amplitude variance. The decreasing shape parameter also indicates an increase in skewness toward low strains.

Feature tracking

Representative feature displacement tracks showing sensitivity of correlation coefficient to cycle-to-cycle displacement differences are given in Fig. 6. Mean correlation coefficients with 25th and 75th percentiles for all tracked points are shown in Fig. 7. Both puncture groups yielded displacement tracks that were significantly less well correlated than control between the first and second and between the second and third cycles. Correlation between the third and fourth cycles was not significantly different between any groups. The 21-G group showed a significant improvement in correlation from the first to second and second to third cycles.

Discussion

Needle injection into the IVD for discography or injection of biologic repair agents results in AF injury. This study developed techniques to measure the microscale impact of needle injection on AF tissue and demonstrated that punctures resulting from the use of even the smallest discography needles alter the local structure of the annulus and compromise its mechanical function. The study used a combination of mechanical loading, confocal microscopy, and digital image processing techniques to look, for the first time, at the micromechanical environment of the IVD AF after needle puncture injury. The findings supported our hypotheses that needle puncture alters local strain patterns by creating a hole with broken fibers leading to regions of strain amplification and strain shielding. Results of this study also demonstrated that this alteration does not propagate with repeated loading at physiological levels. There was no evidence that treatment with genipin, a cross-linking agent, might mitigate the effect of a needle puncture on microscale shear strains.

Several important conclusions can be drawn from the strain amplitude distribution (Fig. 5). The first is a confirmation of the qualitative observation that small areas of large

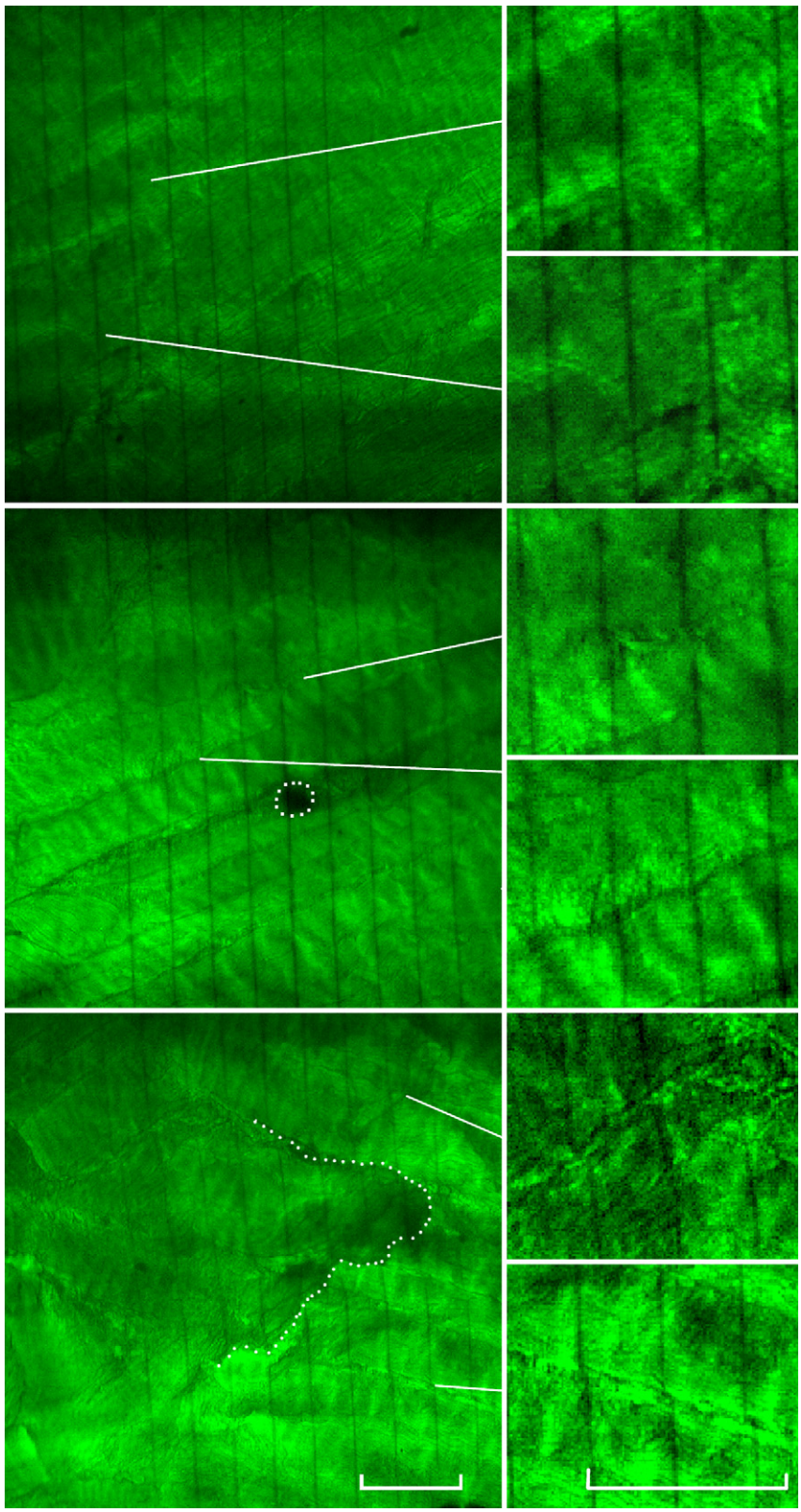

Fig. 3. (Top) Representative micrographs of specimens at maximum shear showing injury morphologies, including undamaged (Middle) small circular hole, and (Bottom) large tear. Dotted lines indicate approximate boundary of primary injury. (Middle and Bottom) Insets have been digitally enhanced to show marker line discontinuity present in punctured specimens (Top) but not control. Scale bars are 250 μm.

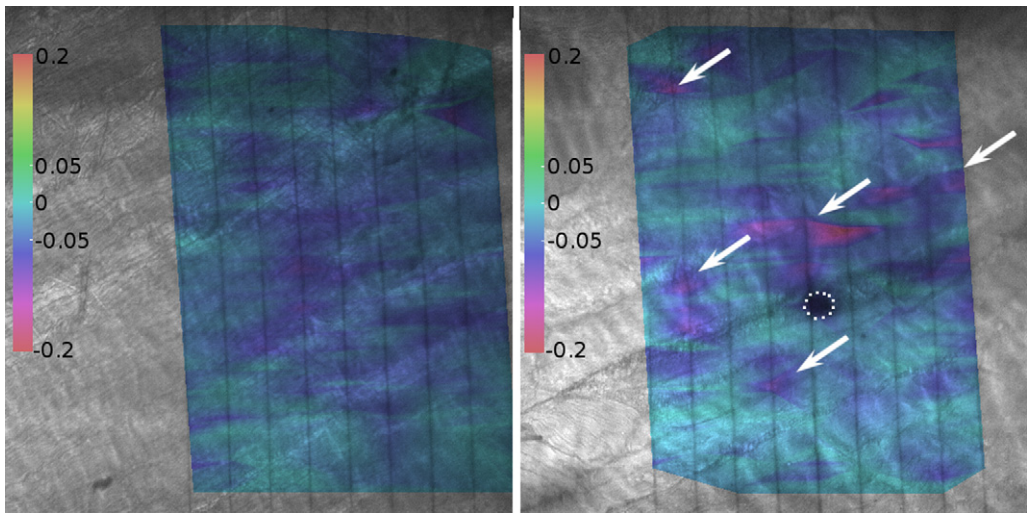

Fig. 4. (Left) Representative strain maps of control, (Right) punctured specimens, showing small areas of increased shear strain (white arrows) along fiber bundle boundaries near puncture (dotted white line).

shear strain occur in the vicinity of the puncture site, which is made apparent by the measurement of strains above 10% in punctured specimens but not in the control specimen. The second is the greatly increased incidence of low strain amplitude measurements, suggesting a corresponding strain-shielding effect. Continuum theory predicts that the introduction of a circular hole into an anisotropic material under shear will disrupt shear strains mostly within a radius of four hole diameters, with increases and decreases in strain dictated by angular location relative to the hole center [22]. The present study confirms that strain disruption is localized to the area immediately around the needle puncture; however, the hierarchical fiber structure of the AF causes strain amplification to occur preferentially at fiber bundle boundaries regardless of angular location. This redistribution from a fairly homogenous strain field to small areas of amplification and large areas of strain shielding may have a critical impact on cellular activity. It has previously been reported by Breuhlmann et al. [38] that sliding between collagen fibrils at a scale of around 10 μm plays an important role in AF cell microenvironment. Concentration of shear strain at both the puncture site and the boundaries between fiber bundles (Fig. 4) likely correspond to an alteration in cell deformation. This alteration in cell deformation may have played a role in previously reported cell death surrounding a needle puncture [12] and long-term increase in degeneration risk [21]. Results suggest that a single local injury acutely puts cells at risk of apoptosis through altered mechanotransduction and may, by itself, initiate a degenerative cascade. It is, therefore, imperative that injuries of this type be minimized or repaired for cells to carry out healthy long-term function.

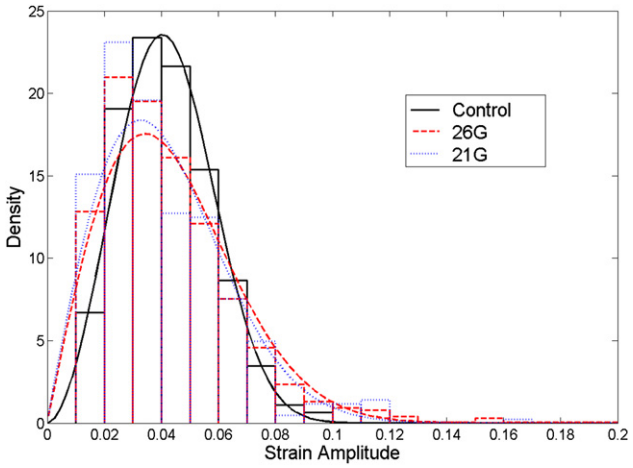

Fig. 5. Histogram of local shear strain amplitudes with lines indicating Weibull functions. (Control: 462 measurements from one specimen, 26 G; 1754 measurements from seven specimens, 21 G; 426 measurements from three specimens).

The most encouraging finding of this study is the ability of AF tissue to arrest the growth of a defect within a low number of cycles of strain at physiological amplitude. This suggests that the cell biological consequences of strain amplification and shielding after needle puncture can be mitigated in some way if the mechanical deficiency is corrected in a timely manner. Genipin alone did not seem to adequately bridge broken AF fibers, but it is possible that cross-linked scaffolds offer more promise.

The choices of animal model and needle sizes made in this study provide a reasonable representation of human discs after injection. The bovine tail IVD exhibits strong similarities in biochemical makeup and AF fiber structure

Table
Parameters of Weibull functions fit to shear strain amplitude distributions shown in Fig. 5

Treatment group	Variance	Scale	Shape
Control	$2.6e^{-4}$	0.047	2.81
26 G	$5.1e^{-4}$	0.049	1.95
21 G	$4.7e^{-4}$	0.050	1.01

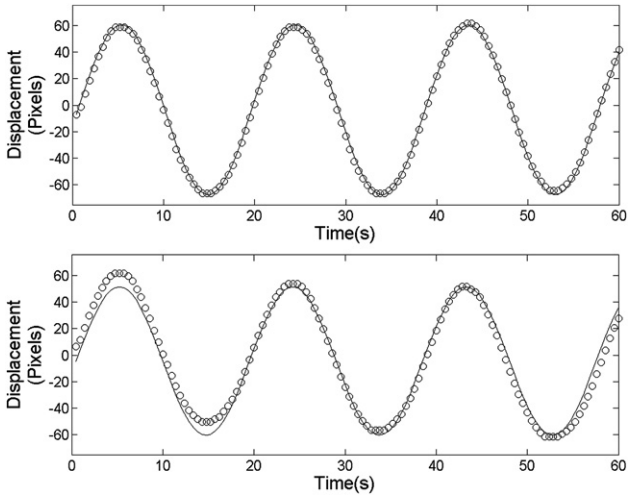

Fig. 6. Representative feature displacement traces (○) with first to second cycle correlation coefficients of (Top) 0.9998 and (Bottom) 0.9996. Sinusoidal fits (–) have been added for comparison.

[43,44] with healthy young human discs. The use of bovine tissue created a model system with low interspecimen variability, allowing for more precise investigation of needle puncture effects and assessment of image processing repeatability [8,45–47]. The use of tissue explants rather than whole discs also minimized the effect of differences in disc geometry between species. Although the testing of tissue explants rather than whole motion segments does not exactly mimic a particular physiological situation, simple shear at the tissue level occurs under most organ-scale motions (torsion, bending, and so on) and may be easily generalized. Needle puncture effects in human disc tissues are important areas of future investigation, which will allow measurements of more complex interactions between needle puncture and existing disc lesions as well as age-related structural changes, such as interlamellar space thickening and derangement of fiber microstructure.

Although the Radon transform technique used in this study has great potential for measuring the angles and rotations of line features on deformed tissues, it does have some limitations. In particular is the case where measurements may be made on areas, where line features have moved out of focus. Analysis of white noise found a bias toward 180° when a line feature is not present, which is likely an artifact of performing a polar transform on square pixels. When line features are distinct, the measurement is reliable, but precision is limited by the width and sharpness of the line relative to the size of the subwindow. These techniques do, however, offer a visual and quantitative means of assessing localized tissue damage.

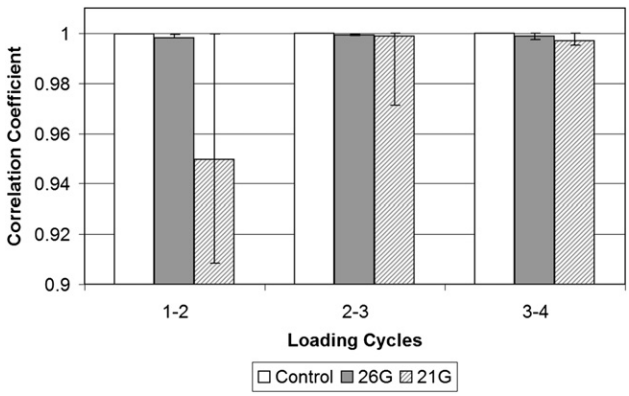

Fig. 7. Mean correlation coefficients between point displacements through successive cycles of applied shear. Error bars indicate 25th and 75th percentiles (bars indicate p<.05 between groups).

There is growing evidence that needle injection from discography can predispose IVDs to degeneration [21], and this study provides a potential biomechanical mechanism for this clinical observation. Needle puncture injury results in distinct patterns of disruption of the normal micromechanical environment of the IVD AF under circumferential shear. Needle injuries resulted in circular holes and larger more jagged tears and were not correlated with needle size in the range tested. These injuries are unlikely to self-repair because of the low metabolic activity of AF cells. The resulting changes in micromechanical strain environment may impact tissue stresses and local cellular environment providing a mechanism for accelerated degeneration of punctured discs. However, physiological levels of dynamic shear were not found to significantly propagate needle puncture injuries beyond the first two cycles of loading because of the robust fiber-reinforced laminated structure of the annulus, suggesting that the injury may be repairable. Genipin treatment alone was not effective at mitigating the effects of puncture injury, and future repair strategies should focus on directly bridging broken fibers, which will likely require a fiber-reinforced hydrogel rather than a simple cross-linking agent.

References

[1] Urban JPG, Roberts S. Degeneration of the intervertebral disc. Arthritis Res Ther 2003;5:120–30.
[2] Guyer RD, Ohnmeiss DD. Lumbar discography. Spine J 2003; 3(3 Suppl):11S–27S.
[3] Fenton DS, Czervionke LF. Image-guided spine intervention. 1st ed. Philadelphia, PA: Saunders, 2003.
[4] Miyamoto K, Masuda K, Kim JG, et al. Intradiscal injections of osteogenic protein-1 restore the viscoelastic properties of degenerated intervertebral discs. Spine J 2006;6:692–703.
[5] Ho G, Leung VY, Cheung KM, Chan D. Effect of severity of intervertebral disc injury on mesenchymal stem cell-based regeneration. Connect Tissue Res 2008;49:15–21.
[6] Evans C. Potential biologic therapies for the intervertebral disc. J Bone Joint Surg Am 2006;88(2 Suppl):95–8.
[7] Masuda K, Imai Y, Okuma M, et al. Osteogenic protein-1 injection into a degenerated disc induces the restoration of disc height and structural changes in the rabbit anular puncture model. Spine 2006;31:742–54.
[8] An HS, Takegami K, Kamada H, et al. Intradiscal administration of osteogenic protein-1 increases intervertebral disc height and proteoglycan content in the nucleus pulposus in normal adolescent rabbits. Spine 2005;30:25–31; discussion 31–2.

[9] Iatridis JC, Michalek AJ, Purmessur D, Korecki CL. Localized intervertebral disc injury leads to organ level changes in structure, cellularity, and biosynthesis. Cell and Mol Bioeng 2009;2:437–47.
[10] Aoki Y, Akeda K, An H, et al. Nerve fiber ingrowth into scar tissue formed following nucleus pulposus extrusion in the rabbit anular-puncture disc degeneration model: effects of depth of puncture. Spine 2006;31:E774–80.
[11] Kim KS, Yoon ST, Li J, et al. Disc degeneration in the rabbit: a biochemical and radiological comparison between four disc injury models. Spine 2005;30:33–7.
[12] Korecki CL, Costi JJ, Iatridis JC. Needle puncture injury affects intervertebral disc mechanics and biology in an organ culture model. Spine 2008;33:235–41.
[13] Sobajima S, Kompel JF, Kim JS, et al. A slowly progressive and reproducible animal model of intervertebral disc degeneration characterized by MRI, X-ray, and histology. Spine 2005;30:15–24.
[14] Elliott DM, Yerramalli CS, Beckstein JC, et al. The effect of relative needle diameter in puncture and sham injection animal models of degeneration. Spine 2008;33:588–96.
[15] Hsieh AH, Hwang D, Ryan DA, et al. Degenerative anular changes induced by puncture are associated with insufficiency of disc biomechanical function. Spine 2009;34:998–1005.
[16] Michalek JL, Funabashi KL, Iatridis JC. Needle puncture injury of the rat intervertebral disc affects torsional and compressive biomechanics differently. Eur Spine J 2010 Jun 11. [Epub ahead of print].
[17] Wang JL, Tsai YC, Wang YH. The leakage pathway and effect of needle gauge on degree of disc injury post anular puncture: a comparative study using aged human and adolescent porcine discs. Spine 2007;32:1809–15.
[18] Han B, Zhu K, Li FC, et al. A simple disc degeneration model induced by percutaneous needle puncture in the rat tail. Spine 2008;33:1925–34.
[19] Zhang H, La Marca F, Hollister SJ, et al. Developing consistently reproducible intervertebral disc degeneration at rat caudal spine by using needle puncture. J Neurosurg Spine 2009;10:522–30.
[20] Masuda K, Aota Y, Muehleman C, et al. A novel rabbit model of mild, reproducible disc degeneration by an anulus needle puncture: correlation between the degree of disc injury and radiological and histological appearances of disc degeneration. Spine 2005;30:5–14.
[21] Carragee EJ, Don AS, Hurwitz EL, et al. 2009 ISSLS Prize Winner: Does discography cause accelerated progression of degeneration changes in the lumbar disc: a ten-year matched cohort study. Spine 2009;34:2338–45.
[22] Lekhnitskii SG. Theory of elasticity of an anisotropic elastic body. In: Brandstatter JJ, ed. Holden-day series in mathematical physics. San Francisco, CA: Holden Day, 1963.
[23] Rannou F, Richette P, Benallaoua M, et al. Cyclic tensile stretch modulates proteoglycan production by intervertebral disc annulus fibrosus cells through production of nitrite oxide. J Cell Biochem 2003;90:148–57.
[24] Rannou F, Lee TS, Zhou RH, et al. Intervertebral disc degeneration: the role of the mitochondrial pathway in annulus fibrosus cell apoptosis induced by overload. Am J Pathol 2004;164:915–24.
[25] Rannou F, Poiraudeau S, Foltz V, et al. Monolayer anulus fibrosus cell cultures in a mechanically active environment: local culture condition adaptations and cell phenotype study. J Lab Clin Med 2000;136:412–21.
[26] Neidlinger-Wilke C, Wurtz K, Liedert A, et al. A three-dimensional collagen matrix as a suitable culture system for the comparison of cyclic strain and hydrostatic pressure effects on intervertebral disc cells. J Neurosurg Spine 2005;2:457–65.
[27] Miyamoto H, Doita M, Nishida K, et al. Effects of cyclic mechanical stress on the production of inflammatory agents by nucleus pulposus and anulus fibrosus derived cells in vitro. Spine 2006;31:4–9.
[28] Matsumoto T, Kawakami M, Kuribayashi K, et al. Cyclic mechanical stretch stress increases the growth rate and collagen synthesis of nucleus pulposus cells in vitro. Spine 1999;24:315–9.
[29] Vernon-Roberts B, Moore RJ, Fraser RD. The natural history of age-related disc degeneration—the pathology and sequelae of tears. Spine 2007;32:2797–804.
[30] Michalek AJ, Buckley MR, Bonassar LJ, et al. Measurement of local strain in intervertebral disc anulus fibrosus tissue under dynamic shear: contributions of matrix fiber orientation and elastin content. J Biomech 2009;42:2279–85.
[31] Pezowicz CA, Robertson PA, Broom ND. Intralamellar relationships within the collagenous architecture of the annulus fibrosus imaged in its fully hydrated state. J Anat 2005;207:299–312.
[32] Pezowicz CA, Robertson PA, Broom ND. The structural basis of interlamellar cohesion in the intervertebral disc wall. J Anat 2006; 208:317–30.
[33] Yerramalli CS, Chou AI, Miller GJ, et al. The effect of nucleus pulposus crosslinking and glycosaminoglycan degradation on disc mechanical function. Biomech Model Mechanobiol 2007; 6:13–20.
[34] Hedman TP, Saito H, Vo C, Chuang SY. Exogenous cross-linking increases the stability of spinal motion segments. Spine 2006;31: E480–5.
[35] Chuang SY, Lin LC, Tsai YC, Wang JL. Exogenous crosslinking recovers the functional integrity of intervertebral disc secondary to a stab injury. J Biomed Mater Res A 2010;92:297–302.
[36] Chuang SY, Odono RM, Hedman TP. Effects of exogenous crosslinking on in vitro tensile and compressive moduli of lumbar intervertebral discs. Clin Biomech (Bristol, Avon) 2007;22:14–20.
[37] Krahn KN, Bouten CV, van Tuijl S, et al. Fluorescently labeled collagen binding proteins allow specific visualization of collagen in tissues and live cell culture. Anal Biochem 2006;350:177–85.
[38] Bruehlmann SB, Matyas JR, Duncan NA. ISSLS prize winner: collagen fibril sliding governs cell mechanics in the anulus fibrosus—an in situ confocal microscopy study of bovine discs. Spine 2004;29: 2612–20.
[39] Buckley MR, Gleghorn JP, Bonassar LJ, Cohen I. Mapping the depth dependence of shear properties in articular cartilage. J Biomech 2008;41:2430–7.
[40] Krismer M, Haid C, Rabl W. The contribution of anulus fibers to torque resistance. Spine 1996;21:2551–7.
[41] Adams MA, Hutton WC. The relevance of torsion to the mechanical derangement of the lumbar spine. Spine 1981;6:241–8.
[42] Ramm AG, Katsevich AI. The Radon transform and local tomography. New York, NY: CRC Press, 1996.
[43] Demers CN, Antoniou J, Mwale F. Value and limitations of using the bovine tail as a model for the human lumbar spine. Spine 2004;29: 2793–9.
[44] Yu J, Winlove PC, Roberts S, Urban JP. Elastic fibre organization in the intervertebral discs of the bovine tail. J Anat 2002;201:465–75.
[45] Marchand F, Ahmed AM. Investigation of the laminate structure of lumbar disc anulus fibrosus. Spine 1990;15:402–10.
[46] Cassidy JJ, Hiltner A, Baer E. Hierarchical structure of the intervertebral disc. Connect Tissue Res 1989;23:75–88.
[47] Stokes IA, Iatridis JC. Mechanical conditions that accelerate intervertebral disc degeneration: overload versus immobilization. Spine 2004;29:2724–32.